Advances in Colloid and Interface Science 303 (2022) 102640

Contents lists available at ScienceDirect

Advances in Colloid and Interface Science

journal homepage: www.elsevier.com/locate/cis

Historical Perspective

Nanoparticles: From synthesis to applications and beyond

Atiđa Selmani [a,*], Davor Kovačević [b], Klemen Bohinc [c,*]

[a] Department of Pharmaceutical Technology and Biopharmacy, Institute of Pharmaceutical Sciences, University of Graz, 8010 Graz, Austria
[b] Division of Physical Chemistry, Department of Chemistry, Faculty of Science, University of Zagreb, Horvatovac 102a, 10000 Zagreb, Croatia
[c] Faculty of Health Sciences, University of Ljubljana, Zdravstvena pot 5, SI-1000 Ljubljana, Slovenia

ARTICLE INFO

Keywords:
Synthesis of nanoparticles
Characterization of nanoparticles
Stability of nanoparticles
Charge regulation
Drug delivery
Nanomedicine

ABSTRACT

In modern-day research, nanoparticles (size < 100 nm) are an indispensable tool for various applications, especially in the field of biomedicine. Although enormous efforts have been made to understand the properties and specificities of nanoparticles, many questions are still not answered and the new ones arise. In this review we summarize current trends in the nanoparticle synthesis and characterization and interpret the stability of nanoparticles in various media from aqueous solutions to biological milieu important for the *in vitro* and *in vivo* studies. To get more detailed insight into nanoparticle charging properties and interactions of nanoparticles with interfaces the theoretical models are presented. Finally, the overview of nanoparticle applications is given and the future prospects are discussed.

1. Introduction

Nanoparticles (NPs) are commonly defined as particles with the size of 100 nm or smaller in at least one dimension. It is important to point out that NPs display unique and often improved physico-chemical properties in comparison to the corresponding bulk material. While bulk materials commonly have constant physical properties regardless of their size, the size of nanoparticles dictates their physical and chemical properties. NPs have attracted huge attention due to their small size and high surface to volume ratio that give rise to their reactivity and extraordinary chemical, electronic, optical, magnetic, and mechanic properties. Nanotechnology is a platform that enables design, manipulation and tailoring of the physico-chemical properties of NPs such as size, shape, surface charge and hydrophilicity [1].

There are plenty of ways how to divide nanoparticles. One of these is to divide them in three groups regarding their chemical composition: i) organic (liposomes, dendrimers, micelles, and polymeric hydrogel nanoparticles), ii) inorganic (metals, metal oxides, ceramics, zeolites, and quantum dots), iii) and carbon-based NPs [2].

Various strategies for the NPs synthesis are based on the top-down and bottom-up synthesis. In the top-down approach, the size of the bulk material is reduced to fine NPs by breaking down into their monomers, while the NPs in the bottom-up synthesis are build up from the atom. Various chemical, physical and recently biological techniques are utilized for the NPs fabrication. The literature survey reveals that many publications focus on the static batch synthesis or on the usage of multiple pathways for the NPs production [3]. The non-scalable production hinders the translation from batch to clinical applications. Since the interest for the green and more sustainable NPs fabrication is increased, the development of modern nanotechnologies provides the switch from the "trial and error" batch synthesis, that displays the differences from batch to batch synthesis, to the versatile continuous NPs production. The high-throughput flow techniques (*i.e.* microfluidic techniques) enable the controlled NPs production that overcomes the variability and generates NPs with high uniformity [4].

Besides the synthesis that should provide NPs with desired properties, the characterization of the engineered NPs is an essential step in the NPs manufacturing. In this context, numerous methods are used for the determination of their physico-chemical properties such as composition, crystal structure, size, shape, surface charge, morphology and specific surface area. Such comprehensive characterization of the surface properties enables the prediction of NP's behaviour at the various interfaces.

A very important aspect in studying the properties and applications of nanoparticles is their behaviour in various matrices (*e.g.* biological fluids). When charged, nanoparticles come in contact with electrolyte solution the electric double layer is formed by NP attraction of a cloud of oppositely charged ions. H. von Helmholtz proposed a very simple description of the electric double layer model in which he assumed that counterions electrostatically adsorb on the NPs surface leading to a compact layer of counterions. In addition to electrostatics, Gouy and

* Corresponding authors.
E-mail addresses: atida.selmani@uni-graz.at (A. Selmani), klemen.bohinc@zf.uni-lj.si (K. Bohinc).

https://doi.org/10.1016/j.cis.2022.102640
Received 30 December 2021; Received in revised form 4 March 2022; Accepted 6 March 2022
Available online 10 March 2022

Chapman included the entropic disorder of ions. This theoretical approach is named Poisson-Boltzmann (PB) theory and is based on the mean-field approximation, where all types of correlations are neglected. The ions are point-like and embedded in a continuum electrolyte solution with a given dielectric constant. The charge on the NP's surface is continuously smeared. For monovalent ions and weakly charged NPs, the PB theory makes correct predictions for ion concentration around charged NP's surfaces [5]. In the past there were many attempts to improve the classical PB theory by considering general charge distribution on the NPs surface and NPs finite size [6–8]. The charge regulation was incorporated into the PB theory by mass action law [9] where the reactions taking place on the NP's surfaces are considered [10].

In terms of possible applications of nanoparticles, a very important moment is a requirement for having a stable dispersion of nanoparticles. The stability of nanoparticles is related to the suspension properties such as pH, concentration and shape of nanoparticles and ionic strength [11,12]. It is important to stress here that especially the complexity of the biological matrices (in terms of pH, ionic strength and the presence of biological macromolecules such as proteins, lipids, enzymes) triggers the stability of NPs. This is highly relevant for the NPs behaviour *in vivo*, where the abovementioned biomolecules adsorb on NPs when in contact with biological fluids [13]. The adsorbed biological molecules on NP surface lead to the so "called protein-corona" complex (PC) formation and the primary identity of NPs is changed. The new adopted identity of the PC complex presents a challenge for the effective applications in nanomedicine. However, that could lead to the development of new platforms for the design and tailoring of the improved nanomedicines.

Nanoparticles recently emerged also as an innovative and promising platform for the development of the drugs and drug delivery vehicles in the modern medicine. Therefore, the possible applications of NPs in field of biomedicine could be found in the diagnostics, treatment, and prevention of the diseases. NPs are already commonly used in medical imaging, gene and drug delivery, detection of pathogens and proteins, tissue engineering, *etc.* [14].

The aim of this review is to provide a general overview on the state-of-the-art in the field of nanoparticles synthesis, characterization and applications with special emphasis on the possibilities for obtaining the improved stability of NPs. The charge regulation of nanoparticles and their interactions with interfaces are also discussed.

2. Synthesis and characterization of nanoparticles

The highly demanding criteria in the fabrication of the NPs is the optimization of the synthesis processes that yield NPs with defined size, monodispersity, surface charge and morphology. The physico-chemical properties of NPs have the crucial role for the *in vivo* fate of NPs, since they dramatically alter their *in vivo* performance in terms of absorption, pharmacokinetics, and clearance, cellular uptake and cytotoxicity [15]. There are numerous techniques available for the NPs synthesis. Each approach gives versatile NPs that differ in size, shape (spheres, nanowires, nanotubes, nanosheets, nanoplates, nanodiscs, nanoflowers, etc), dimensionality (0D, 1D, 2D or 3D), crystallinity, and surface area. NPs performance in various applications is strongly influenced by all the mentioned parameters. NPs can be prepared by two approaches: i) top-down approach referring to a stepwise breaking down of a system into nanosized entities and ii) bottom-up approach meaning the build-up from the atomic or molecular size to form the nanomaterial (Fig. 1). The top-down approach requires precise control of the pressure, temperature and inert environment where the process takes place. However, the output of the top-down approach are the nanomaterials with variation in size, shape and surface defects that affects their application. The bottom-up approach displayed nanomaterials with better control of size, crystallinity, morphology and reproducibility.

The classical chemical synthesis methods for NPs can be divided in three categories regarding the media where reaction take place: solution-based, gas-based and bio-assisted synthesis methods as shown in Fig. 1. The chemical methods comprise the solution-based techniques: co-precipitation, sol-gel synthesis, solvothermal/hydrothermal synthesis, microwave-assisted method, sonochemical, microemulsion synthesis and electrochemical synthesis.

The formation of NPs by co-precipitation method [16,17] involves mixing of divalent or trivalent salt precursors, usually chlorides and nitrates as a metal ion source with a base (NaOH, KOH or NH_4OH solution). The formation of NPs by co-precipitation method involves nucleation, growth, Ostwald ripening and agglomeration. The precipitates are subjected to calcination at the elevated temperature to obtain final nanomaterial. Sol-gel synthesis [18,19] is based on the hydrolysis of metal alkoxide precursors to form oxohydroxide. This reaction is followed by the polycondensation, and the sol phase of the

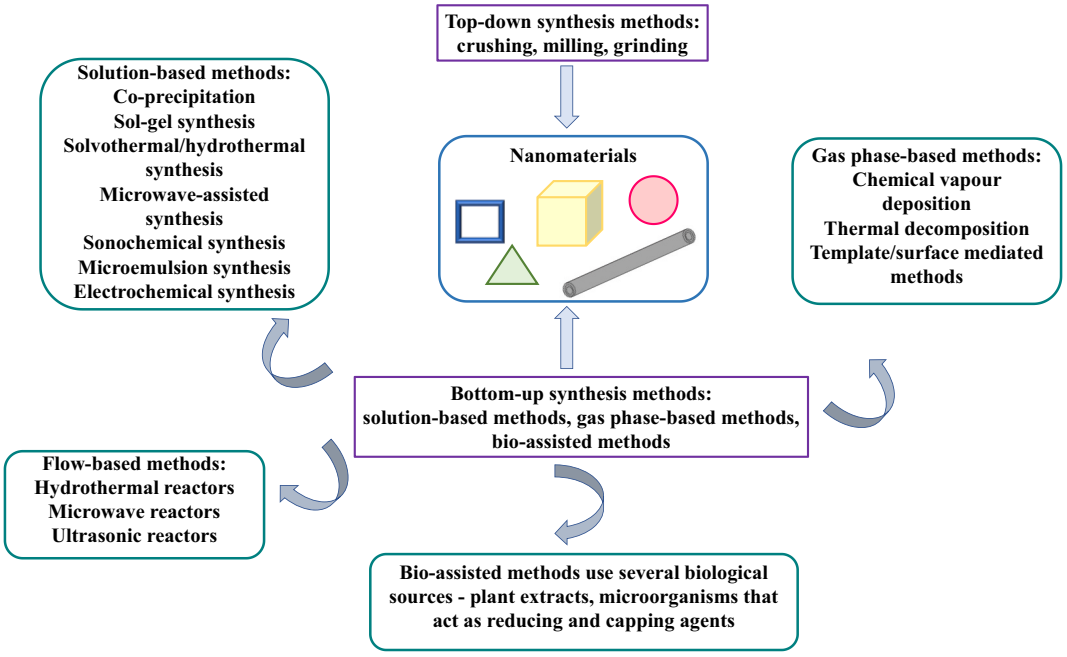

Fig. 1. Workflow for the methods for the nanomaterial's synthesis.

mixture is transformed into the porous gel phase and forms a metal hydroxide network. The calcination of the obtained gel leads to the ultra-fine powdered NPs. Solvothermal/hydrothermal method [20,21] is based on the thermal decomposition of the starting metallic precursor by boiling in the inert atmosphere or in the closed system, *i.e.* Teflon-lined autoclave at high pressure and temperature. Solvothermal approach is distinguished from the hydrothermal by reaction medium, *i.e.* solvothermal synthesis is conducted in the organic solvents, while the hydrothermal synthesis in aqueous medium. The hydrothermal synthesis method is of often method of choice for the production of homogenous NPs with desired properties which can be improved by post-synthesis treatments such as annealing. Microwave-assisted [22,23] synthesis received a great attention recently, due to shorter reaction duration in comparison to for example oil-bath heating. This synthesis method is based on the fast and uniform heating of the reaction solution, which is achieved *via* penetration of the microwave energy through the walls of the reactor. The rapid heating increases the collision frequency between molecules and chemical reaction rate, leading to dramatically decrease of the reaction duration from hours to minutes. In this way, the uniform nucleation and fast crystal growth is enabled, resulting in NPs with smaller uniform size. Sonochemical method [24,25] corresponds to the application of the high-power ultrasound waves (20 kHz–10 MHz) to the reaction solution. The reaction solution is subjected to the stream of the ultrasound waves that produces bubbles (cavities) through acoustic cavitation in the liquid medium. The acoustic cavitation involves bubble formation, growth and implosive bubble collapse, followed by the emergence of high-energy shock waves inside the collapsing bubble. The energy released by huge number of the collapsing bubbles is followed by the temperature increase (5000 K–25000 K) that is sufficient to break the chemical bonds of the starting material. The bubbles collapse very fast (< 1 ns) and the high rate of cooling process takes place which favours the amorphous product formation, while the crystallization is disabled. Microemulsion synthesis [26,27] requires formation the micelles or the reverse micelles that serve as the nano-reactors where NPs formation takes place. The microemulsions are transparent, homogenous and thermodynamically stable systems composed of water, oil, surfactant and co-surfactant. The spontaneous mixing between two immiscible phases, water and oil is achieved by formation of a surfactant molecules monolayer at the interface between the oil and water. The co-surfactant is usually short-chain amine or alcohol that increases the fluidity of the interface and reduces the interfacial tension between oil and water, thus enabling the permeability of oil and water phases. Electrochemical synthesis [28,29] is achieved by applying the electric current between electrodes that are separated by an aqueous electrolyte solution. The electrochemical reaction takes place at the interface between electrode and aqueous electrolyte solution. The final product (coatings, thin films or powders) is deposited on the electrode surface.

Gas-phased methods are chemical vapor deposition, thermal decomposition/ thermolysis and template/surface mediated. Chemical vapor deposition [30,31] is a synthesis approach where substrate in the reaction chamber is exposed to gas volatile precursors that are introduced in the reaction chamber. The gas precursors react with substrate and the coated substrate with desired composition is fabricated. The residues produced after the synthesis, are removed by gas-flow through reaction chamber. Thermal decomposition/ thermolysis [32,33] is a method where the metallic precursor in the reaction vessel is heated, heating cause breaking of the chemical bonds of the starting material. The decomposition of the starting material is followed by the formation of the NPs. Metallic precursor is usually salt in form of carbonate or acetate. By addition of the capping agents (surfactants, carboxylic acids and alkyl amines) the NPs are stabilized. Template/surface [34,35] mediated method is used for the synthesis of the nanorods, nanowires nanotubes and hollow spheres. The synthesis of the nanomaterial is conducted within the pores of the nanoporous template. The templates used for this method can be soft templates (surfactants and polymers) and hard templates (polymer microspheres, porous membrane, carbon fiber, carbon nanotubes and porous anodic aluminum oxide). The size, morphology and structure are controlled by the template used for the synthesis.

Bio-assisted methods are based on the green chemistry principles (mild reaction conditions and nontoxic precursors) and usage of biological sources such as bacteria, viruses, fungi, yeast, algae and plant extracts that are nano-factories (Table 1). The bio-assisted synthesis method is using the reduction enzymes and molecules such as polysaccharides, phenolic acids, alkaloids, tannin, terpenoids, polyphenol of the employed biological entities to produce the NPs intracellularly or extracellularly. The biological source extract serves as the reduction agent of the metallic starting material as well the capping agent that stabilize the NPs and prevents their aggregation.

The conventional "trial" and "error" nanoparticle synthesis (*e.g.* non-continuous bulk synthesis), mostly done in academic research, is limited due to batch-to-batch reproducibility. However, this approach represents the foundation for the better understanding and optimization of the scaling-up processes for the industrial needs. The high-throughput production, *e.g.* continuous production of NPs with controllable physico-chemical properties still presents a challenging task but also the most crucial step for the efficient translation of the nanomedicines from the academic batch-based research to an industry large-scale production. The state-of-the-art in the NPs production and the alternative for the versatile NPs synthesis are continuous flow techniques, *e.g.* microfluidic reactors. The main driving force in the microfluidic reactors is hydrodynamic force. The stable flow profile, *e.g.* laminar flow in the channels is determined by the delicate interplay between inertial, viscous and interfacial forces [50]. The fluid flow in the microfluidic reactor depends on the channel geometry, properties of the fluids and flow conditions [51]. Microfluidic reactors serve as the platform developed to control fluid flow in the microreactors by minimization of the reagents volume, facilitate efficient transfer of mass and heart due to large surface to volume ratio and increase the mixing rates at the interface between two phases [52]. The precise control and modification of the synthesis conditions (volume, temperature, pH, duration of the reaction), process parameters (flow rate of the reactants, total flow rate, method for the energy transfer) and the microreactor characteristics (inlet design, length, diameter) define the final NPs properties in selective manner so they can meet the quality control criteria for the further application [53].

Nanomaterials display unique physico-chemical properties such as crystallinity and composition, morphology, size, and surface properties with promising application in various fields. The NPs are then subjected to conjugation with polymers, proteins, drugs, *etc.* that alter the initial NP properties. The available state-of-the-art techniques give the insight

Table 1
Selected examples for the bio-assisted synthesis of the NPs.

Biological source	Biological extract	NPs	Size(nm)/Shape	Ref
Plant	*Asparagus racemosus* root	Fe_2O_3	30–40 / spherical	[36]
	Plantain peel	Fe_3O_4	50 / spherical	[37]
	Plectranthus amboinicus leaf	ZnO	50–180 / rod-like	[38]
	Calotropis gigantean leaf	ZnO	10 / spherical	[39]
	Annona squamosal peel	TiO_2	25 / spherical	[40]
	Moringa oleifera peel	CeO_2	45 / spherical	[41]
	Hibiscus Sabdariffa flower	CdO	113 / cuboid	[42]
	Kalopanax pictus leaf	MnO_2	20 / spherical	[43]
	Carica papaya leaf	CuO	140 / rod-like	[44]
Algae	*Gracilaria edulis*	ZnO	65–95 / rod-like	[45]
	Sargassum muticum	Fe_3O_4	20 / cube-like	[46]
Bacteria	*Aeromonas hydrophila*	ZnO	60 / spherical	[47]
	Bacillus subtilis	TiO_2	75 / spherical	[48]
	Microbacterium sp. MRS-1	NiO	100–500 / flower-like	[49]

about the relevant parameters in order to describe the physico-chemical properties in detail for the further application (Table 2). The crystal structure and composition of fabricated NPs is the first step in the work flow of the NP characterization. Many available techniques such as X-ray diffraction (XRD), Fourier-transform infrared (FTIR) and Raman spectroscopy, nuclear magnetic resonance (NMR) are the methods of choice to identify the composition, crystal structure and the influence of the coating agent and conjugated drug on NP properties. The morphology of NPs significantly affects the interaction with cells and *in vivo* uptake and the microscopy techniques such as scanning (SEM) and transmission electron microscopy, (TEM) as well as atomic force microscopy (AFM) provide detailed insight about NP morphology.

The size and size distribution of NPs that reflects stability in various media relevant for the biomedical application is studied extensively by scattering techniques (static (SLS) and dynamic light scattering, (DLS), nanoparticle tracking analysis (NTA), small-angle X-ray scattering (SAXS) but also with support of microscopy-based techniques. The surface charge of NPs is the crucial parameter for the estimation of the interaction with cells. When in contact with biological fluids, NPs interact with the biological molecules and lose their identity. Determination of surface charge (*i.e.* zeta potential) upon the incubation with biological fluids with electrophoretic light scattering (ELS) or streaming potential methods is fast and robust way to predict the NP behaviour and stability. The concentration of NPs as well their dissolution upon exposure with biological fluids is a critical step that determine their uptake and toxicity. Despite the numerous experimental techniques available for the NPs characterization, to the best of our knowledge, there are no tandem or integrated techniques available to asses all of the relevant NPs physico-chemical properties simultaneously. This multi-method set-up with powerful analytical detection platforms would significantly improve quality control of the NPs.

3. Stability of nanoparticles and their interactions with macromolecules

A very vital issue related to the application of nanoparticles is a requirement for their stable dispersion. Due to the large specific surface area, nanoparticles tend to agglomerate over time which results in a separation of the dispersed phase from the continuous phase [65]. The stability of nanoparticles could be manipulated through changes in various stimuli, allowing a transition between the stable dispersion and aggregated clusters [66]. That is particularly relevant if experiments are intended to be performed at physiological pH or in complex biological fluids. It is well known that the stability of nanoparticles, in addition to pH and ionic strength of the solution, depends on the intrinsic properties of NPs (*e.g.* size, shape, surface charge, porosity, roughness, hydrophobicity) [67].

Table 2
The most common techniques for NPs characterization.

	Technique	Analytical information	Reference
Electron microscopy	TEM	morphology, elemental composition, size	[54]
	SEM	morphology, size	[55]
Spectroscopy	XRD	composition, crystal structure, crystallite size	[56]
	FTIR	surface chemical composition, nature of bonds and functionality	[55]
	Raman	chemical structure, crystallinity and molecular interactions.	[57]
	UV–Vis	optical properties, size, concentration, agglomeration of NPs	[58]
Scattering techniques	DLS	size, size distribution, agglomeration of NPs	[59]
	NTA	size and size distribution	[60]
	SAXS	size, size distribution, growth kinetics	[61]
Surface charge determination	ELS	zeta potential	[62]
	streaming potential	zeta potential	[63]
Surface analysis	BET	specific surface area	[64]

Various pathways are being used for stabilization of nanoparticles. Previously, low-molecular organic compounds (*e.g.* carbonic acids, alcohols, amides) and natural polymers (*e.g.* gelatin, gum arabic, cellulose) were commonly used. Later on, synthetic polymers were also used [68]. For example, it was shown recently that suspensions of metal oxide nanoparticles could be stabilized using lipid-based nanovesicles (liposomes) [69] or aminopolycarboxylic acids [70]. In this sense, one of the most promising tools for stabilization of nanoparticles is the adsorption of polyelectrolytes [71]. In terms of applications it should be stressed here that polyelectrolyte-stabilized Pt nanoparticles were applied as new electrocatalysts for low temperature fuel cells [72]. Moreover, Seal and coworkers studied the stability of ceria nanoparticles induced by adsorption of weak polyanion polyacrylic acid (PAA) and showed that PAA-coated ceria nanoparticles efficaciously preserved the stability and surface chemistry of nanoparticles [73]. Oćwieja, Adamczyk and coworkers showed that polyelectrolytes could also be applied as the layers that enable the pronounced stability of *e.g.* silver nanoparticle coatings [74]. Such effects have also practical implications indicating the possibility to regulate the rate of nanoparticle release by a proper choice of the polyelectrolyte acting as the supporting layer. The same authors showed additionally that polyelectrolyte-modified polystyrene microparticles could be used as substrates for silver nanoparticle immobilization [75]. In that case, a large stability of the silver particle monolayers was confirmed. Such monolayers of well-defined coverage and acid-base properties can be used for controlled delivery of silver nanoparticles.

The influence of polyelectrolytes on the stability of nanoparticles was additionally explored in our recent study [12] where the interactions of ceria nanoparticles with a strong polyanion, sodium poly (4-styrenesulfonate) were examined. For the interpretation of the experimental results obtained in our study we applied electrophoretic soft particles model, so called modified Ohshima model based on the measurements of mobility, μ, of nanoparticles coated with a polyelectrolyte layer. The expression for the mobility derived by Ohshima [76,77] is given by

$$\mu = \frac{\varepsilon_0 \varepsilon_r}{\eta} \frac{\frac{\psi_0}{\kappa_m} + \frac{\psi_{DON}}{\lambda}}{\frac{1}{\kappa_m} + \frac{1}{\lambda}} f\left(\frac{D_{coated}}{D_{CNP}}\right) + \frac{ZeN}{\eta\lambda^2} \quad (1)$$

where ε_r and ε_0 represent the relative permittivity and the permittivity of the free space, respectively, e is the elementary charge, η is the viscosity of solvent, κ_m is a modified Debye parameter accounting for the effect of charges in the polyelectrolyte layer, and $f(D_{coated}/D_{CNP})$ is a function which ranges from 2/3 to 1. The number density and valence of charge present on polyelectrolyte-coated layer are denoted by N and Z, respectively, while surface potential at the boundary between the surface layer and the surrounding electrolyte solution and the Donnan potential are represented by ψ_0 and ψ_{DON}, respectively. The diameter of the bare nanoparticle is denoted by D_{CNP} and the diameter of polyelectrolyte-coated nanoparticles is represented by D_{coated}. Finally, δ presents the thickness of the polyelectrolyte layer, as schematically presented in Fig. 2.

The interpretation of the results on the basis of the Ohshima model leads to the value of the electrophoretic softness (*i.e.* the softness of the polyelectrolyte layer) of $1/\lambda = 3.03$ nm, while the charge density of the polyelectrolyte is equal to $ZeN = -0.032$ mol dm^{-3}. Finally, the adsorption density of polyelectrolyte on nanoparticle surface [73] was obtained using the equation

$$\Gamma = N \frac{(D_{CNP} + 2\delta)^3}{(D_{CNP})^2} M \quad (2)$$

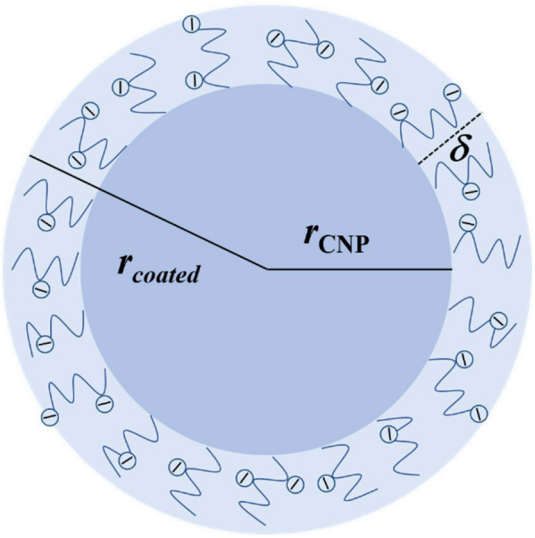

Fig. 2. Schematic presentation of the model applied for the interpretation of adsorption of polyelectrolytes on spherical NPs; radii of the bare nanoparticle and of polyelectrolyte-coated nanoparticle are denoted by r_{CNP} and r_{coated}, respectively, while δ presents the thickness of the polyelectrolyte layer.

where Γ represents the adsorption density and M is monomer molar mass. On the basis of performed experiments and calculations the adsorption density of polyelectrolyte adsorption on ceria nanoparticles was found to be $\Gamma = (5.42 \pm 2.73)$ mg m^{-2}.

The importance of presented adsorption experiments combined with appropriate interpretation lies in possible predictions of the behaviour of nanoparticles in polyelectrolyte solution in terms of known values of adsorption density and electrophoretic softness. These findings could enable the preparation of suspensions having satisfactory stability which could lead to the improved applications of nanoparticles in various research fields.

The stability of nanoparticles in the complex biological matrices and their internalization within cells is a delicate interplay between intrinsic NP properties (*e.g.* size, shape, surface charge, hydrophobicity, porosity) and external biological characteristics of the medium (pH, ionic strength, temperature, composition and concentration of the biological molecules) as shown in Fig. 3. The intrinsic NP properties could be tuned during the synthesis, but also afterwards with post-treatment procedures. However, the unpredictable and uncontrollable interactions with biological molecules alter the stability and final fate of NPs.

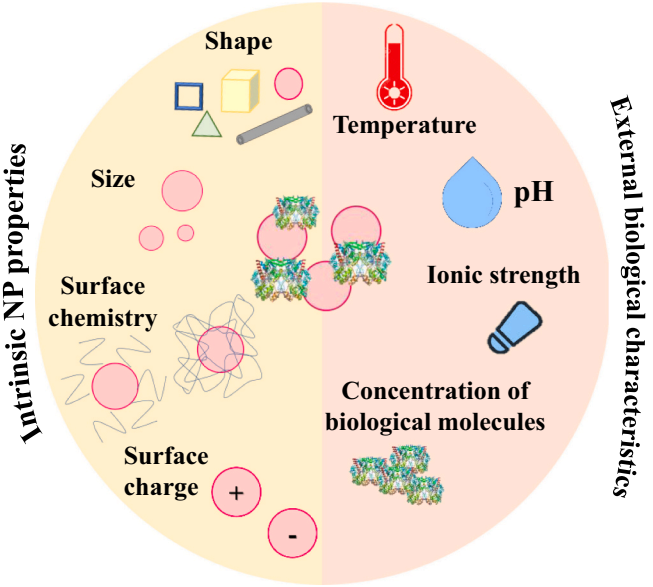

Fig. 3. The intrinsic NP properties and external biological characteristics that affect the stability of NPs in the biological media.

NPs in contact with biomolecules form a layer on the surface of NPs (*e.g.* protein corona), and NPs-PC complex is formed [78]. PC screens the surface of NPs and affects the cellular uptake, circulation lifetime, signaling, kinetics, transport, accumulation, toxicity and immune response [79]. The nano/bio interface, *i.e.* NPs-PC complex, is an interactive and dynamically changeable interface. The number of reactions and interactions that occur at the nano/bio interface are still challenging to describe. It is established that NPs-PC complex reduces the efficacy of NPs as the drug delivery vehicle. Recent published data are oriented to *in vitro* studies which enable the insight on the interactions between NPs and biological molecules, but often fail to the predict and explain the fate of NPs *in vivo* [80,81]. The complexity of *in vivo* studies is the limiting factor for understanding the special events that occur between NPs and biomolecules and for the further progress in the field of nanomedicine.

4. Charge regulation

Most nanoparticles are charged and immersed in an electrolyte solution. The generic structure for many of NPs is a body of low dielectric constant with attached surface charges. The charges at the surface are fixed or mobile. Some NPs possess charged moieties that have a complex internal structure. The generic structure of the electrolyte solution is an ensemble of ions and water molecules leading to a high dielectric constant of the solution ($\varepsilon = 80$). NPs attract ions of the opposite charge sign. These ions are called counterions, while ions of the same charge sign as NPs are called coions and are depleted from NPs. A diffusive electric double layer arises [82].

Metal oxide surfaces of NPs are charged due to interactions between active surface sites and two types of ions: protons H^+ and hydroxide ions OH^- [83]. In the simplest case, the surface charge of NPs is the result of the two-step protonation of active surface groups (Fig. 4)

$$\equiv MO^- + H^+ \rightarrow \equiv MOH \quad (3)$$

$$\equiv MOH + H^+ \rightarrow MOH_2^+ \quad (4)$$

The corresponding thermodynamic equilibrium constants of the surface reactions are K_1 and K_2.

The spatial distribution of mobile ions near NPs can be predicted by the classical Poisson-Boltzmann theory, which is based on a mean-field approximation where correlations due to steric effects and fluctuations are neglected. Within the Poisson-Boltzmann theory the free energy F can be written as [5]

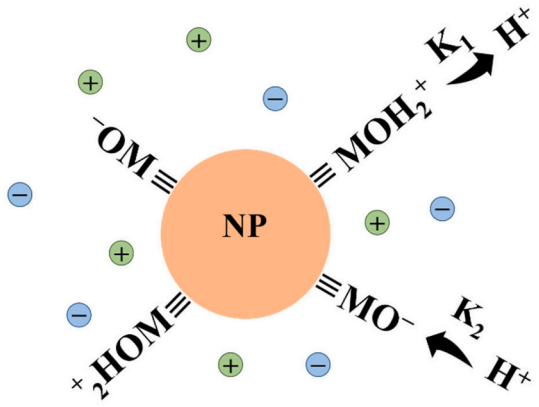

Fig. 4. Surface reactions at the NPs/aqueous media interface.

$$F = \frac{1}{8\pi\, l_B}\int_V (\nabla\psi)^2 \mathrm{d}V + k_B T \int_V \sum_{i=1}^{N} (n_i ln n_i / n_{0i} - n_i + n_{0i})\mathrm{d}V \quad (5)$$

where the first term on the rhs of Eq. (5) corresponds to the energy associated with the presence of an electrostatic field $\vec{E} = -\nabla\phi$, where ϕ is the electrostatic potential, ∇ is the nabla operator and $\psi = e\phi/k_B T$ is the reduced electrostatic potential, with $k_B T$ being the thermal energy. The second term corresponds to the translational entropy contributions of ions coions and counterions in the aqueous solution. The ion concentration of the i-th type is denoted as n_i and the sum goes through all ion species from 1 to N. n_{0i} are the ion bulk concentrations. The integrals go through the full space V. The distance between two elementary charges at which their Coulomb interaction equals the thermal energy is the Bjerrum length l_B.

In thermodynamic equilibrium the free energy functional $F(\psi, n_i)$ adopts a minimum with respect to the electrostatic potential and ion concentrations. The minimization procedure of F results into Boltzmann distributions for ion concentrations which are inserted into Poisson equation leading to the Poisson-Boltzmann equation for the electrostatic potential ψ [5]

$$\frac{\mathrm{d}^2\psi(r)}{\mathrm{d}r^2} + \frac{a}{r}\frac{\mathrm{d}\psi(r)}{\mathrm{d}r} = -4\,\pi l_B \sum_i z_i n_{0i}\, e^{-z_i\psi(r)} \quad (6)$$

where z_i is the ion valency of the i-th species. The parameter a is connected with the geometry, for spherical NPs $a = 2$, for cylindrical NPs $a = 1$ and for planar NPs $a = 0$. The differential Eq. (4) can be solved together with two boundary conditions

$$\frac{\mathrm{d}\psi}{\mathrm{d}r}(r = R) = -4\pi\, l_B \frac{\sigma}{e} \quad (7)$$

$$\psi(\infty) = 0 \quad (8)$$

which follows from the electro-neutrality of the system. The last boundary condition fixes the electrostatic potential to zero far from the charged surface. The surface charge density σ is

$$\sigma = \sum_{k=1}^{M} \Gamma_k e\, z_k \quad (9)$$

where Γ_k is the surface site concentration of the charged group of the k-th type. The sum runs over all type of charged groups on the NPs from $k = 1$ to M.

The charge regulation is especially important to understand and interpret the experimental data of the NP's charge. Fig. 5. shows the surface charge density as a function of pH for three different adsorption site densities. At lower pH the NP's surfaces are positively charged whereas at higher pH the surfaces are negatively charged.

The finite size of ions is especially pronounced close to NPs surface

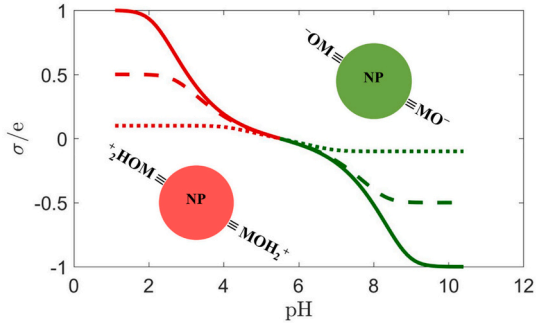

Fig. 5. Surface charge density σ as a function of pH for three different adsorption site densities Γ. The calculation was made for spherical NPs. The salt concentration is 2 mM.

[84]. Stern has improved the PB theory by dividing the electric double layer into two domains, one that encompasses a shell of adsorbed counterions and another one that represents the diffusive part of the electric double layer in the vicinity of the NP's surface. The lattice gas and Carnahan-Starling equations of state are the two most frequently used self-consistent approaches to incorporate excluded volume interactions.

Efforts to consider correlations were made in two ways: strong and weak electrostatic couplings [85]. The former case is very relevant for multivalent ions. Shklovskii proposed an approximate method to describe inter-ionic correlations through the formation of a Wiegner crystal. The weak correlation regime is connected to the modification of the classical PB theory: integral-equation theories, perturbative expansions around the classical PB model, local density-functional theory, and field theoretic methods. Intra-ionic correlations need to be introduced in the case of ions or molecules with spatially distributed charge [86].

To verify some of the predictions of the present modified PB model against computational results, Monte Carlo (MC) simulations need to be performed including electrostatic and short-range interactions. The results of Monte Carlo simulations are ionic distribution profiles along with some thermodynamic quantities (excess internal energy and chemical potential of ions). One of the aims of computer simulations is to verify validity range of the modified Poisson-Boltzmann theory. More realistic models in terms of shape and positions of charged groups on NPs can be modeled. Molecular dynamics (MD) simulations can also deliver important insight of the system. Compared to MC simulations MD simulations can give a more detailed prospect of the complicated systems. MD simulations are also very useful to describe biological systems where water ordering plays a very important role.

5. Interactions between nanoparticles and interfaces

Interactions between nanoparticles and interfaces in aqueous solutions (Fig. 6) play an important role in different fields of science that find applications in a wide variety of fields, including paints, ceramics, drug dispersions, soils or food processing. The charged interfaces could be lipid membranes, mica, DNA, colloids, metal oxides, actin molecules, proteins, viruses, and even cells. The charge structure of NP and their internal degrees of freedom as well as charge structure of interfaces influence the interaction strength between NP and different type of interfaces [8,87,88].

The following mechanisms of the interface charging exist: the preferential adsorption/desorption of the surface lattice ions, specific adsorption of ions, ionization of surface functional groups, isomorphic substitution and accumulation/depletion of electrons at the surfaces. Most of these cases can be considered as described in subsection 4. Here we consider an example of the structured surface, which includes groups with spatially extended charge. The simplest case of such groups is zwitterionic lipid consisting of a negatively charge phosphate group at the polar-apolar interface and a positively charged choline or ethanolamine group. Both entities are separated by a distance l. The contribution to the free energy of the zwitterionic lipid layer (in addition to eq. 5) is [95]

$$F_{\mathrm{lipid}} = k_B T\,(1-\varphi)\,\frac{1}{l}\int_0^l W(x) ln W(x)\mathrm{d}x \quad (10)$$

This term is the entropic contribution of the zwitterion's orientational degree of freedom. The fraction of charged lipids is denoted by φ and $W(x)$ is the conditional probability density for the terminating charge of the zwitterionic lipids to be located at x. Let's note that in this case the functional depends also on the conditional probability density $F(\psi, n_i, P)$.The functional needs also to be minimized with respect to W leading to the modified Boltzmann distribution.

NPs have generally different charge distributions on the surface. In recent studies, we approximate NPs by charged spherical particles with

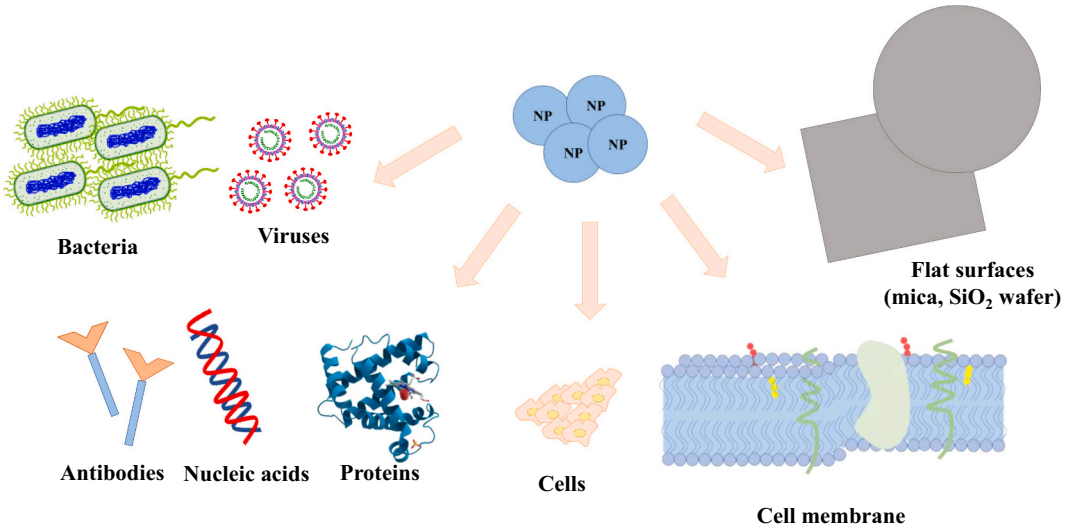

Fig. 6. Interaction between NPs and different interfaces: bacteria, viruses, metal oxide surfaces, cells, antibodies, nucleic acids and proteins.

discrete and continuous charge distributions. The classical PB theory has been generalized to consider the system of nanoparticles near charged interfaces [6,89,90,91,92].

$$\frac{F}{Ak_BT} = \frac{1}{8\pi l_B}\int_{-\infty}^{\infty} \mathrm{d}x\, \Psi'(x)^2 + \int_{-\infty}^{\infty} \mathrm{d}x \frac{1}{2l}\int_{-l}^{l} \mathrm{d}s\, n(x,s)[lnn(x,s)v - 1 - U(x,s)] \tag{11}$$

where the ion distribution function $n(x, s)$ is defined as joint probability for the positional and orientational degrees of freedom. Integration over all possible orientations s gives the concentration function of NPs

$$n(x) = \int_{-l}^{l} n(x,s)\mathrm{d}s \tag{12}$$

The external potential $U(x, s)$ prevents that NPs cannot penetrate through the charged walls. The results of theoretical considerations are the electrostatic potential, concentration profiles, orientation profiles and equilibrium free energy. A large impact is made by the salt addition. The results showed that the attractive interactions between like charged interfaces corroborates the possibility of condensation induced by NPs with spatially distributed charges. The attractive force between like charged interfaces is the result of intra-ionic correlations introduced through the uniform surface charge density of the NPs. Inter-ionic correlations can further enhance the degree of attraction. The increasing salt concentration of the system has a large influence on the surface charge screening and on the concentration of nanoparticles close to the charged surface. The salt addition decreases the nematic order parameter of NPs [7,93,94].

Interactions between NPs and lipid layers are especially important from biological point of view where all possible orientational degrees of freedom and shapes can be considered. Recently we showed that the adsorption of NPs onto the lipid layer is mainly driven by the electrostatic interactions [95,96]. Similar effects were observed also with DNA adsorption onto lipid layers.

Electrostatic interactions affect the immersion depth of NPs trapped at an air water interface. Experiments showed that upon adding salt negatively charged NPs penetrate deeper into the water. The positively charged NPs exhibit opposite quite behaviour. In agreement with experiments, the modified PB theory predicts opposite behaviors of negatively *versus* positively charged NPs: adding salt increases/decreases the water immersion depth of NPs with negative/positive charge [97].

6. Applications

Recent advances in the synthesis, characterization and interpretation procedures related to nanoparticles presented in previous chapters facilitated the production of versatile and high-quality NPs. The structure, size, antioxidative and catalytic properties, biocompatibility, permeability and prolonged retention time at the targeted place of delivery of such NPs enabled their widespread usage in the various scientific fields, primarily in biomedicine, biosensing and bioimaging applications (Fig. 7). The numerous options are available for tailoring and improving the physico-chemical properties of NPs. That allows the design of more efficient nano-based drug delivery systems that have predetermined surface properties, size distribution and morphology for the controlled therapeutic efficiency [98].

Biomedicine is demanding sophisticated high-throughput nano drug delivery systems that are safe and efficient. The promising options are nanomedicines based on the rational design of pharmacologically active multifunctional nano-scale drug delivery systems that consider nano-bio interactions and appropriate biological response. The development of targeted nano-scale drug delivery systems enables the establishment of innovative platforms for the improvement of already existing medicines or design of the novel therapeutics' strategies. NPs conjugated or functionalized with anticancer drugs, peptides, proteins, genes or vaccines display enhanced activity and therapeutic effect. Smaller dose, efficient response and low systemic toxicity are the key elements for overcoming the intrinsic limitations of drugs [99]. Currently, state-of-the-art in the precise NPs engineering is oriented towards the design of personal nanotherapeutics, *i.e.* personal medicine that could overcome the patient heterogeneity, one of the main limits of the traditional medicine [100]. In addition, an efficient drug delivery vehicle should avoid rapid clearance of the reticuloendothelial system, pass across biological barriers and overcome the pharmacokinetic limitations related with associated conventional medicines. Many studies are oriented towards the development of nanomedicines that could improve patient's response to applied therapy. These nanomedicines are based on the innovative strategies that fabricate engineered NPs with precise properties. Moreover, the patient's medical history is also taken into account. The combined approach facilitates the progress towards the personalized therapy that is the main goal in the advanced nano-therapy.

Inorganic NPs such as mesoporous silica, as well as iron, titanium and zinc oxides, display strong potential for the applications in the biomedical fields such as diagnostics, theranostics and therapy. In this section the overview of selected NPs and their biomedical applications

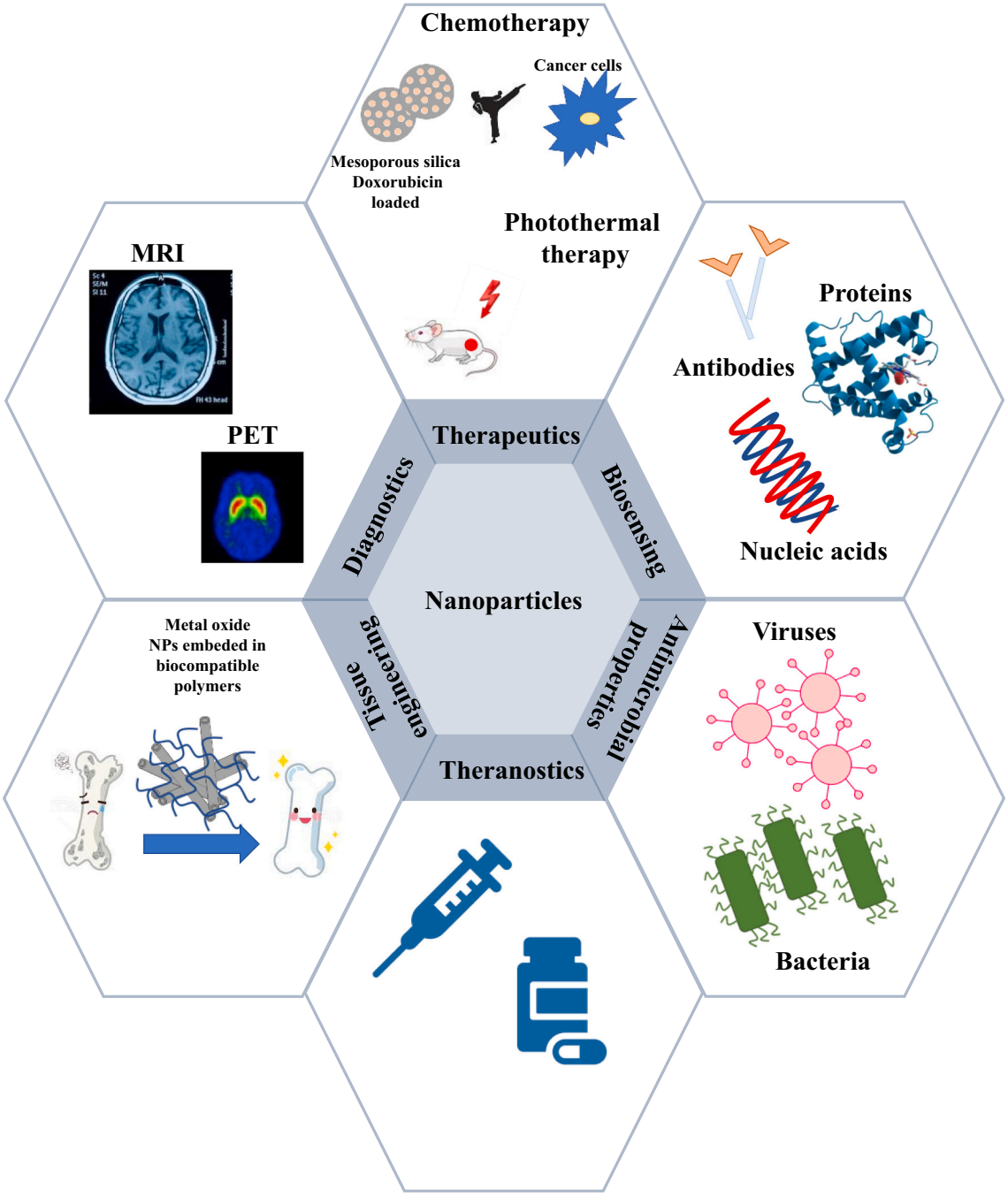

Fig. 7. Overview of NP applications in the fields of biomedicine, biosensing and bioimaging.

will be presented.

Mesoporous silica nanoparticles (MSNs), as highly ordered structures containing large pores with uniform porous dimensions ranging from 2 to 50 nm, are among the most exploited nano-platforms with huge potential for the biomedical applications [101]. The extraordinary intrinsic properties and high loading capacity of MSNs, together with their physical and chemical functionalization, enhanced the biocompatibility of such nanoparticles. All of that, including their interactions and conjugation with biomolecules, promoted MSNs as the candidates with extraordinary biomedical potential [102–107]. Ren et al. developed nanoreactors for multi-synergistic cancer therapy comprised of MSNs-palladium (SP) and doxorubicin-cyclodextrin complex (pDOX-CD) [108]. Design of that nanoreactor is based on glucose oxidase (GOD) mediated cancer starvation therapy, $H_2O_2^-$ mediated orchestrated oxidation therapy and DOX induced chemotherapy [109,110] (Fig. 8).

Liu and co-workers prepared sustainable reactive oxygen species (ROS) generator by encapsulation of nano-sized manganese tetroxide-chlorine e6 conjugates (Mn_3O_4-Ce6) into dendritic MSNs followed by coating with hyaluronic acid for the photodynamic therapy (PDT) [111]. The sustainable ROS generator required for the PDT presents an innovative strategy for enhanced ROS-mediated anti-cancer therapy.

Magnetic iron oxide NPs (IONPs; maghemite, γ-Fe_2O_3 and magnetite, Fe_3O_4) are extensively exploited in biomedicine due to their specific properties that provide size-dependent magnetic targeting. They are nontoxic, biocompatible and biodegradable [112]. Iron oxide NPs are widely used as contrast agents for magnetic resonance imaging (MRI), in magnetic hyperthermia treatment, for drug and cell targeting and as nanozymes due to intrinsic enzyme-like activity [113–115]. Li et al.

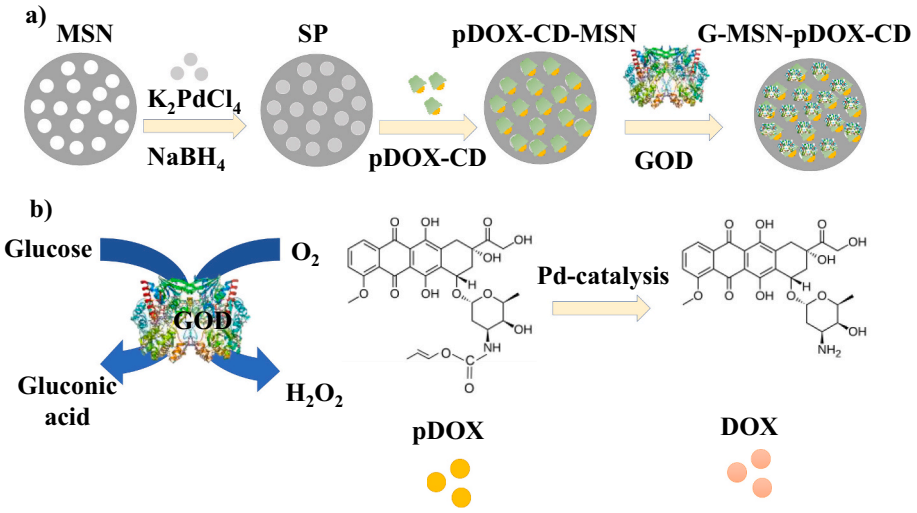

Fig. 8. Design of the nanoreactor based on palladium-doxorubicin-cyclodextrin complex and MSNs activated *in situ* by the combination of glucose oxidase activity and palladium to achieve multi-synergistic cancer therapy. Copyright permission from American Chemical Society. Figure adopted and modified from Ren et al. [108].

fabricated polydopamine functionalized Fe_3O_4 nano-composites for the MRI-guided photothermal therapy (PTT) cancer treatments [116]. Polydopamine coating enabled improved biocompatibility, stability and photothermal response. The nanocomposite exhibits long-term stability, excellent MRI contrast enhancement effect and performance. *In vivo* studies on 4 T1 tumor-bearing mice display high antitumor activity where tumors were removed which represents a great potential for the further clinical applications. IONPs functionalized with metronidazole-conjugated dendrons which are used as radiopharmaceuticals that recognize hypoxia in tumors was prepared by Filippi et al. [117]. The biological activity of metronidazole, *i.e.* tracing of hypoxia within cells and tissues combined with IOPNs could facilitate MRI diagnosis and tumor recognition. *In vitro* studies showed that obtained NPs are biocompatible with negligible cytotoxic effect, they favour bio-interactions and selectively accumulate in the less oxygenated tissue. The developed innovative theranostic nanoplatform enables the active recognition of hypoxia levels and safe and versatile imaging and diagnostics that can distinguish normal *vs* hypoxic tissues.

Titanium oxide (TiO_2) NPs have attracted significant interest among scientists due to their biocompatibility, chemical stability, photocatalytic properties and plethora of shapes that find usage in numerous applications in the fields such as biosensing, medical implants, drug delivery and antibacterial applications [118]. In addition, the possibility to generate ROS in the presence of UV-light and damage cancer cells has a huge potential in various therapies. Multimodal TiO_2 nanocorals with light-triggered drug release for the cancer chemotherapy were developed by Yadav et al. [119]. It was shown that the amount of released DOX can be tuned by UV-light irradiation which can be used for the further development of the TiO_2 NPs as the light-triggered drug delivery system for cancer treatment. Ge and co-workers fabricated gold/carbon/TiO_2 (Au@C/TiO_2) nanorod array photoelectrochemical glucose biosensor [120]. Photoelectrochemical biosensors have attracted huge interest due to many advantages like low noise to signal ratio, low cost and high sensitivity. The photoactive properties of the semiconductor determine the sensitivity of the sensor. Combination of Au, C and TiO_2 nanorods immobilized with glucose oxidase displayed good stability and reproducibility and excellent efficiency for the glucose detection.

Zinc oxide (ZnO) NPs also emerged recently as promising drug delivery systems as presented in the study by Ghaffaria and co-workers [121]. Curcumin loaded zinc oxide, ZnO-β-CD nanoflowers functionalized with mercaptopropionic acid and conjugated with folic acid were designed to enhance the distribution, targeting, bioavailability and release profile of curcumin into breast cancer cells. The overexpressed folate receptor has been found in many tumors and serves as a biomarker for the cancer cells. Therefore, design of many advanced drug delivery vehicles includes conjugation of folic acid that targets the folate receptor which results in elevated anti-cancer drug uptake and improved anti-cancer efficacy. Briones et al. reported fluorometric ZnO nanowires-enzyme bioconjugate assay for the lactate and cholesterol oxidase detection in human serum [122]. Determination of lactate oxidase concentration in serum is of huge importance for the detection of several conditions such as haemorrhage, respiratory failure, hepatic disease, sepsis and tissue hypoxia. Elevated cholesterol level in blood is a biomarker for the cardiovascular diseases, high blood pressure and diabetes type 2. Conventional methods for lactate and cholesterol determination are time-consuming and less accurate. In the presented research fast fluorometric assay is based on the detection of formed hydrogen peroxide during oxidation of lactate or cholesterol. Hydrogen peroxide quench the ZnO nanowires photoluminescence signal, which corresponds to the lactate and cholesterol concentration in the serum. Promising analytical properties, *i.e.* low detection signal, good selectivity and reproducibility, enable development of the high-throughput nanoplatforms for the future applications in the detection of lactate and cholesterol in various samples.

Besides their enormous potential in the field of biomedicine, NPs emerged as the antiviral and antibacterial functional agents. NPs multimodal mechanism against microbe's homeostasis is comprised of direct interaction with the bacterial cell wall or a capsid in viruses, inhibition of the biofilm formation, release of metal ions, triggering reactive ROS formation, interference with DNA or protein synthesis [123]. Nanoparticles are also advantageous in treating bacterial infections and can be used in antibacterial coatings for implants and medicinal materials to prevent infection, as well as for promoting wound healing [124–127].

Valuable information about the possible applications of coated NPs as antibacterial coatings could be deduced from the corresponding systems containing metal oxide plates or similar surfaces. For example, polyelectrolyte multilayers (PEMs) could influence the promotion or the disruption of the bacterial biofilm due to their high surface charge density. If the terminating layer of a PEM has an opposite charge than bacteria, the interaction between bacteria and PEM is promoted. In the recent study, we showed that the PEMs formed of poly(allylamine hydrochloride) and sodium poly(4-styrenesulfonate) could increase the antibacterial properties of a surface [128]. On the other hand, in the case where the terminated layer of a PEM is a protein, bacterial adhesion

strongly depends on the specificity of the used protein, while the surface physical properties do not play the key role in the adhesion process [129]. Finally, we studied also the bacterial adhesion capacity of uropathogenic *Escherichia coli* to PEM-coated urinary catheter surface [130]. It was shown that the biofilm is easily formed on non-treated PVC surfaces, which was not the case for multilayer coated surfaces. PEM terminating with sodium poly(4-styrenesulfonate) layer showed the lowest bacterial adhesion which could be helpful in prevention of biofilm formation.

Since 2020, the world is facing the Covid-19 pandemic caused by the SARS-CoV-19 virus. The nanotechnology addresses numerous issues related with Covid-19 infection. The multifunctional antiviral coatings, sensors that detect Covid-19 and self-cleaning personal protective equipment based on the NPs displays high potential against it [131–133]. Recent publications highlight sensors based on gold NPs as the efficient tool for the diagnosis of Covid-19 infection [134,135]. Covid-19 virus remain on the surfaces (plastic and steel) for a longer period of time, thus giving rise to infections. Copper and coper oxide NPs covered surfaces display significant antibacterial and antiviral activity through copper ions release and triggering the ROS production [136,137]. The photocatalytic activity of TiO_2 NPs can be used for deactivation of Covid-19 through UV-radiation [138,139]. Even though NPs displayed promising potential against Covid-19, more research has to be done in order to alleviate the serious consequences on the global health. The aim is to capture and inhibit the virus before it infects the host and to prevent the mutation of the virus. The prevention and controlling of the current Covid-19 outbreak, but also issues related to antibiotics resistance, are currently one of the highest priorities in science and modern medicine. Nanotechnology, as a highly versatile platform, displays great potential for the development of antiviral and antibacterial agents that could mitigate the current health crisis.

7. Conclusions and future prospects

In this article we attempted to give an insight into the contemporary state-of-the-art in the field of NP's synthesis, characterization and applications, with a special emphasis on the benefits that could be gained from theoretical considerations of NPs in solution and at the interfaces. In modern science it is indispensable to combine the efforts of the scientists dealing with experimental and theoretical approaches on various topics. It is especially important to find a theoretical model that can adequately describe systematically obtained experimental data. We showed earlier [9] on the example of cerium oxide NPs that the dependence of experimentally obtained surface charge density of truncated octahedron CeO_2 NPs on pH is in a good agreement with the results obtained by the density functional theory. Such a holistic approach that relates the experiment with the theory could significantly contribute to a profounder understanding of the investigated systems. These results could even provide a framework for various tuned applications, especially in the field of biomedicine.

Regarding the future prospects in the field of nanoparticles it should be stated that currently the focus in the NPs production and translation from bench to bedside, is a design and development of the personalized nanomedicine. The precise tuning of NP properties which enables the transport through biological barriers, their conjugation with drugs, antibodies, proteins, nucleic acids, *etc.*, in combination with genetic profile of patient and patient's medical history could generate NPs for the individual treatment. This strategy could greatly improve the drug delivery and patient's response in the applied therapy.

Declaration of Competing Interest

The authors declare that there is no conflict of interest.

Acknowledgement

K.B. thanks the Slovenian Research Agency for the support through program P3-0388. K.B. and D.K. acknowledge the Slovenian Research Agency for the financial support through project J7-2595 and the Croatian Science Foundation for the financial support through project IPS-2020-01-6126.

References

[1] Conde J, Dias JT, Grazú V, Moros M, Baptista PV, de la Fuente J. Front Chem 2014;15(2). https://doi.org/10.3389/fchem.2014.00048.
[2] De Matteis V, Rinaldi R. In: Saquib Q, Faisal M, Al-Khedhairy A, Alatar A, editors. Advances in experimental medicine and biology. Cham: Springer International Publishing; 2018. p. 1–19.
[3] Darr JA, Zhang J, Makwana NM, Weng X. Chem Rev 2017;117:11125. https://doi.org/10.1021/acs.chemrev.6b00417.
[4] Shepherd SJ, Issadore D, Mitchell MJ. Biomaterials 2021;274:120826. https://doi.org/10.1016/j.biomaterials.2021.120826.
[5] Bohinc K, Volpe Bossa G, May S. Adv Colloid Interface Sci 2017;249:220. https://doi.org/10.1016/j.cis.2017.05.001.
[6] Bohinc K, Lue L. J Nanosci Nanotechnol 2015;15(5):3468. https://doi.org/10.1166/jnn.2015.9866.
[7] Bohinc K, Volpe Bossa G, Gavryushov S, May S. J Chem Phys 2016;145:234901. https://doi.org/10.1063/1.4968210.
[8] Spada S, Gavryushov S, Bohinc K. J Mol Liq 2018;270:178. https://doi.org/10.1016/j.molliq.2018.01.139.
[9] Bohinc K, Korade K, Jerin K, Lešić N, Đaković M, Dražić G, et al. ACS Appl Nano Mater 2021;4:1434. https://doi.org/10.1021/acsanm.0c02960.
[10] Špadina M, Gourdin-Bertin S, Dražić G, Selmani A, Dufreche JF, Bohinc K. ACS Appl Mater Interfaces 2018;10:13130. https://doi.org/10.1021/acsami.7b18737.
[11] Keller AA, Wang H, Zhou D, Lenihan HS, Cherr G, Cardinale BJ, et al. Environ Sci Technol 2010;44:1962. https://doi.org/10.1021/es902987d.
[12] Brkljača Z, Lešić N, Bertović K, Dražić G, Bohinc K, Kovačević D. J Phys Chem C 2018;122:27323. https://doi.org/10.1021/acs.jpcc.8b07115.
[13] Berardi A, Baldelli Bombell F. Expert Opin Drug Deliv 2019. https://doi.org/10.1080/17425247.2019.1610384.
[14] Salata OV. J Nanobiotechnology 2004;2:1. https://doi.org/10.1186/1477-3155-2-3.
[15] Shin SW, Song IH, Um SH. Nanomaterials 2015;5(3):1351. https://doi.org/10.3390/nano5031351.
[16] Radoń A, Drygała A, Hawełek L, Łukowie D. Mater Charact 2017;131:148. https://doi.org/10.1016/j.matchar.2017.06.034.
[17] Yousaf S, Zulfiqar S, Shahi MN, Warsi MF, Al-Khalli NF, Aboud MFA, et al. Ceram Int 2020;46:3750. https://doi.org/10.1016/j.ceramint.2019.10.097.
[18] Bao Y, Kang QL, Liu C, Ma JZ. Mater Lett 2018;214:272. https://doi.org/10.1016/j.matlet.2017.12.038.
[19] Possato GL, Pereira E, Gonçalves RGE, Pulcinelli SH, Martins L, Santilli CV. Catalysis Today 2020;344:52. https://doi.org/10.1016/j.cattod.2018.10.027.
[20] Selmani A, Špadina M, Plodinec M, Delač Marion I, Willinger MG, Lützenkirchen J, et al. J Phys Chem C 2015;119:19729. https://doi.org/10.1021/acs.jpcc.5b02027.
[21] Lv Y, Zhang Z, Yan J, Zhao W, Zhai C, Liu J. J Alloys Compd 2017;718:161. https://doi.org/10.1016/j.jallcom.2017.05.075.
[22] Korosi L, Bognar B, Bouderias S, Castelli A, Scarpellini A, Pasquale L, et al. Appl Surf Sci 2019:493. https://doi.org/10.1016/j.apsusc.2019.06.259.
[23] Pelicano CM, Yanagi H. Appl Surf Sci 2020;506:144917. https://doi.org/10.1016/j.apsusc.2019.144917.
[24] Gupta A, Srivastava R. Ultrason Sonochem 2018;41:47. https://doi.org/10.1016/j.ultsonch.2017.09.029.
[25] Ghiyasiyan-Arani M, Salavati-Niasari M, Naseh S. Ultrason Sonochem 2017;39:494. https://doi.org/10.1016/j.ultsonch.2017.05.025.
[26] Munoz-Batista MJ, Ferrer M, Fernandez-Garcia M, Kubacka A. Appl Catal B 2014;154:350. https://doi.org/10.1016/j.apcatb.2014.02.038.
[27] Chen D, Yu Q, Xiang X, Chen M, Chen Z, Song S, et al. Electrochim Acta 2015;154:83. https://doi.org/10.1016/j.electacta.2014.12.037.
[28] Anand V, Srivastava VM. J Alloys Compd 2015;636:288. https://doi.org/10.1016/j.jallcom.2015.02.189.
[29] Fajaroh F, Setyawan H, Widiyastuti W, Winardi S. Adv Powder Technol 2012;23:328. https://doi.org/10.1016/j.apt.2011.04.007.
[30] Li D, Goullet A, Carette M, Granier A, Landesman JP. Mater Chem Phys 2016;182:409. https://doi.org/10.1016/j.matchemphys.2016.07.049.
[31] Escalante G, Juárez H, Fernández P. Adv Powder Technol 2017;28:23. https://doi.org/10.1016/j.apt.2016.07.005.
[32] Bokhonov BB, Matvienko AA, Gerasimov KB, Dudina DV. Ceram Int 2019;45:19684. https://doi.org/10.1016/j.ceramint.2019.06.219.
[33] Khalaji AD, Jarosova M, Machek P, Chen K, Xue D. Scr Mater 2020;181:53. https://doi.org/10.1016/j.scriptamat.2020.02.015.
[34] Qutaish H, Tanaka S, Kaneti YV, Lin J, Bando Y, Alshehri AA, et al. Microporous Mesoporous Mater 2018;271:16. https://doi.org/10.1016/j.micromeso.2018.05.015.
[35] Wu B, Wang L, Wu H, Kan K, Zhang G, Xi Y, et al. Microporous Mesoporous Mater 2016;225:154. https://doi.org/10.1016/j.micromeso.2015.12.019.

[36] Kumara PPNV, Pammi SVN, Shameem U. Int J Pharm Drug Anal 2018;6:22.
[37] Venkateswarlu S, Rao YS, Balaji T, Prathima B, Jyothi NVV. Mater Lett 2013;100:241. https://doi.org/10.1016/j.matlet.2013.03.018.
[38] Fu L, Fu Z. Ceram Int 2015;41:2492. https://doi.org/10.1016/j.ceramint.2014.10.069.
[39] Chaudhuri SK, Malodia L. Appl Nanosci 2017;7:501. https://doi.org/10.1007/s13204-017-0586-7.
[40] Roopan SM, Bharathi A, Prabhakarn A, Rahuman AA, Velayutham K, Rajakumar G, et al. Spectrochim Acta Part A Mol Biomol Spectrosc 2012;98:86. https://doi.org/10.1016/j.saa.2012.08.055.
[41] Surendra TV, Roopan SM. J Photochem Photobiol B Biol 2016;161:122. https://doi.org/10.1016/j.jphotobiol.2016.05.019.
[42] Thovhogi N, Park E, Manikandan E, Maaza M, Gurib-Fakim A. J Alloys Compd 2016;655:314. https://doi.org/10.1016/j.jallcom.2015.09.063.
[43] Moon S, Salunke B, Alkotaini B, Sathiyamoorthi E, Kim BS. IET Nanobiotechnol 2015;9:220. https://doi.org/10.1049/iet-nbt.2014.0051.
[44] Sankar R, Manikandan P, Malarvizhi V, Fathima T, Shivashangari KS, Ravikumar V. Spectrochim Acta Part A Mol Biomol Spectrosc 2014;121:746. https://doi.org/10.1016/j.saa.2013.12.020.
[45] Priyadharshini RI, Prasannaraj G, Geetha N, Venkatachalam P. Appl Biochem Biotechnol 2014;174:2777. https://doi.org/10.1007/s12010-014-1225-3.
[46] Mahdavi M, Namvar F, Ahmad MB, Mohamad R. Molecules 2013;18:5954. https://doi.org/10.3390/molecules18055954.
[47] Jayaseelan C, Rahuman AA, Kirthi AV, Marimuthu S, Santhoshkumar T, Bagavan A, et al. Spectrochim Acta Part A Mol Biomol Spectrosc 2012;90:78. https://doi.org/10.1016/j.saa.2012.01.006.
[48] Kirthi AV, Rahuman AA, Rajakumar G, Marimuthu S, Santhoshkumar T, Jayaseelan C, et al. Mater Lett 2011;65:2745. https://doi.org/10.1016/j.matlet.2011.05.077.
[49] Sathyavathi S, Manjula A, Rajendhran J, Gunasekaran P. Bioresour Technol 2014;165:270. https://doi.org/10.1016/j.biortech.2014.03.031.
[50] Liu Y, Chen G, Yue J. J Flow Chem 2020;10:103. https://doi.org/10.1007/s41981-019-00062-9.
[51] Zhao CX, Middelberg APJ. Chem Eng Sci 2011;66:1394. https://doi.org/10.1016/j.ces.2010.08.038.
[52] Sambiagio C, Noël T. Trends Chem 2020;2:92. https://doi.org/10.1016/j.trechm.2019.09.003.
[53] Jiao M, Zeng J, Jing L, Liu C, Gao M. Chem Mater 2015;27:1299. https://doi.org/10.1021/cm504313c.
[54] Li P, Zhou Y, Zhao Z, Xu Q, Wang Q, Xiao M, et al. J Am Chem Soc 2015;137:9547. https://doi.org/10.1021/jacs.5b05926.
[55] Montero Muñoz M, Ramos Ibarra JE, Rodríguez-Páez JE, Teodoro MD, Marques GE, Coaquira J. Phys Chem Chem Phys 2020;22:7329. https://doi.org/10.1039/C9CP06744B.
[56] Abdi El-Sadek MS, Wasly HS, Batoo KM. Appl Phys A 2019;125:283. https://doi.org/10.1007/s00339-019-2576-y.
[57] Keshavarz M, Kassanos P, Tan B, Venkatakrishnan K. Nanoscale Horiz 2020;5:294. https://doi.org/10.1039/C9NH00590K.
[58] Sharda AG, Wright L, Minelli C. Biointerphases 2018;13:061002. https://doi.org/10.1116/1.5054780.
[59] Lai YH, Koo S, Oh SH, Driskell EA, Driskell JD. Anal Methods 2015;7:249. https://doi.org/10.1039/C5AY00674K.
[60] Kim A, Beng Ng W, Bernt W, Cho NJ. Sci Rep 2019;9:2639. https://doi.org/10.1038/s41598-019-38915-x.
[61] Garcia PRAF, Prymak O, Grasmik V, Pappert K, Wlysses W, Otubo L, et al. Nanoscale Adv 2020;2:225. https://doi.org/10.1039/C9NA00569B.
[62] Delgado AV, González-Caballero F, Hunter RJ, Koopal LK, Lyklema J. J Colloid Interface Sci 2007;309(2):194. https://doi.org/10.1016/j.jcis.2006.12.075.
[63] Merai L, Janovak L, Kovacs DS, Szenti I, Vasarhelyi L, Kukovecz A, et al. Anal Bioanal Chem 2020;412:3395. https://doi.org/10.1007/s00216-019-02307-x.
[64] Shivakumara S, Penki TR, Munichandraiah N. Mater Lett 2014;131:100. https://doi.org/10.1016/j.matlet.2014.05.160.
[65] Loza K, Epple M, Maskos M. In: Gehr P, Zellner R, editors. Biological responses to nanoscale particles. vol. 1. Springer International Publishing; 2019 [Chapter 4].
[66] Johnson L, Gray DM, Niezabitowska E, McDonald TO. Nanoscale 2021;13:7879. https://doi.org/10.1039/D1NR01190A.
[67] Keller AA, Wang H, Zhou D, Lenihan HS, Cherr G, Cardinale BJ, et al. Environ Sci Technol 2010;44:1962. https://doi.org/10.1021/es902987d.
[68] Pomogailo AD, Kestelman VN. In: Hull R, Osgood RM, Parisi J, Warlimont H, editors. Metallopolymer nanocomposites. vol. 81. Springer; 2005 [Chapter 3].
[69] Jiménez-Rojo N, Lete MG, Rojas E, Gil D, Valle M, Alonso A, et al. Chem Phys Lipids 2015;191:84. https://doi.org/10.1016/j.chemphyslip.2015.08.012.
[70] Johansson Salazar-Sandoval E, Johansson MKG, Ahniyaz A. RSC Adv 2014;4:9048. https://doi.org/10.1039/C3RA45875J.
[71] Gittins DI, Caruso F. J Phys Chem B 2001;105:6846. https://doi.org/10.1021/jp0111665.
[72] Tian ZQ, Jiang SP, Liu Z, Li L. Electrochem Commun 2007;9:1613. https://doi.org/10.1016/j.elecom.2007.03.006.
[73] Saraf S, Neal CJ, Das S, Barkam S, McCormack R, Seal S. ACS Appl Mater Interfaces 2014;6:5472. https://doi.org/10.1021/am405250g.
[74] Oćwieja M, Adamczyk Z, Morga M, Kubiak K. J Colloid Interface Sci 2015;445:205. https://doi.org/10.1016/j.jcis.2014.12.071.
[75] Lupa D, Adamczyk Z, Oćwieja M, Duraczyńska D. Colloids Surf A Physicochem Eng Asp 2018;554:317. https://doi.org/10.1016/j.colsurfa.2018.06.015.
[76] Ohshima H. Colloid Polym Sci 2007;285:1411. https://doi.org/10.1016/j.cocis.2013.02.003.
[77] Ohshima H. Soft Matter 2012;8:3511. https://doi.org/10.1039/C2SM07160F.
[78] Huang XL, Teng X, Chen D, Tang FQ, He JQ. Biomaterials 2010;31:438. https://doi.org/10.1016/j.biomaterials.2009.09.060.
[79] Khan S, Gupta A, Verma NC, Nandi CK. J Chem Phys 2015;143:164709. https://doi.org/10.1063/1.4934605.
[80] Bertrand N, Grenier P, Mahmoudi M, Lima EM, Appel EA, Dormont F, et al. Nat Commun 2017;8:1. https://doi.org/10.1038/s41467-017-00600-w.
[81] Lu X, Xu P, Ding HM, Yu YS, Huo D, Ma YQ. Nat Commun 2019;10:1. https://doi.org/10.1038/s41467-019-12470-5.
[82] Evans DF, Wennerström H. The colloidal domain: where physics, chemistry, biology and technology meet. New York: Wiley-VCH; 1994. https://doi.org/10.1002/adma.19960080318.
[83] Lützenkirchen J, Preočanin T, Kovačević D, Tomišić V, Lovgren L, Kallay N. Croat Chem Acta 2012;85:391. https://doi.org/10.5562/cca2062.
[84] Macdonald JR. J Electroanal Chem 1987;223:25. https://doi.org/10.1016/0022-0728(87)85249-X.
[85] Vlachy V. Annu Rev Phys Chem 1999;50:145. https://doi.org/10.1146/annurev.physchem.50.1.145.
[86] Bohinc K, Grime JMA, Lue L. Soft Matter 2012;8:5679. https://doi.org/10.1039/C2SM07463J.
[87] Reščič J, Kovačević D, Tomšič M, Jamnik A, Ahualli S, Bohinc K. Langmuir 2014;30(32):9717. https://doi.org/10.1021/la501683t.
[88] Bohinc K, Reščič J, May S. J Mol Liq 2017;228:201. https://doi.org/10.1016/j.molliq.2016.10.087.
[89] Bohinc K, Reščič J, Spada S, May S, Maset S. J Mol Liq 2019;294:1. https://doi.org/10.1016/j.molliq.2019.111134.
[90] Spada S, Maset S, Bohinc K. Int J Mod Phys B 2019;33(10):1793–6578. https://doi.org/10.1142/S0217979219500929.
[91] Urbanija J, Bohinc K, Bellen A, Maset S, Iglič A, Kralj-Iglič V, et al. J Chem Phys 2008;129(10). https://doi.org/10.1063/1.2972980. 105101/1.
[92] May S, Iglič A, Reščič J, Maset S, Bohinc K. J Phys Chem B 2008;112:1685. https://doi.org/10.1021/jp073355e.
[93] Yang Q, Li L, Zhao F, Wang Y, Ye Z, Hua C, et al. Nanomaterials 2020;10(4). https://doi.org/10.3390/nano10040799. 799-1.
[94] Volpe Bossa G, Roth J, Bohinc K, May S. Soft Matter 2016;12(18):4229. https://doi.org/10.1039/C6SM00334F.
[95] Bohinc K, Brezesinski G, May S. Phys Chem Chem Phys 2012;14(30):10613. https://doi.org/10.1039/C2CP40923B.
[96] Bohinc K, Reščič J, May S. J Mol Liq 2017;228:201. https://doi.org/10.1016/j.molliq.2016.10.087.
[97] Shrestha A, Bohinc K, May S. Langmuir 2012;28(40):14301. https://doi.org/10.1021/la303177f.
[98] Bahrami B, Hojjat-Farsang M, Mohammadi H, Anvari E, Ghalamfarsa G, Yousefi M, et al. Immunol Lett 2017;190:64. https://doi.org/10.1016/j.imlet.2017.07.015.
[99] Sanna V, Sechi M. ACS Med Chem Lett 2020;11(6):1069. https://doi.org/10.1021/acsmedchemlett.0c00075.
[100] Mitchell MJ, Billingsley MM, Haley RM, Wechsler ME, Peppas NA, Langer R. Nat Rev Drug Discov 2021;20:101. https://doi.org/10.1038/s41573-020-0090-8.
[101] Li Z, Zhang Y, Feng N. Expert Opin Drug Deliv 2019;16:219. https://doi.org/10.1080/17425247.2019.1575806.
[102] Wang Y, Xie Y, Kilchrist KV, Li J, Duvall CL, Oupický D. ACS Appl Mater Interfaces 2020;12(4):4308. https://doi.org/10.1021/acsami.9b21214.
[103] Li S, Liao R, Sheng X, Luo X, Zhang X, Wen X, et al. Front Oncol 2019;9:696. https://doi.org/10.3389/fonc.2019.00696.
[104] Lei L, Liu Z, Yuan P, JIn R, Wang X, Jiang T, et al. J Mater Chem B 2019. https://doi.org/10.1039/C9TB00025A.
[105] Zhoua X, Liu P, Nie W, Peng C, Tao Li, Qiang L, et al. Int J Biol Macromol 2020;149:116. https://doi.org/10.1016/j.ijbiomac.2020.01.237.
[106] Sun Y, Zhu X, Liu H, Dai Y, Han R, Gao D, et al. ACS Appl Mater Interfaces 2020;12(5):5569. https://doi.org/10.1021/acsami.9b20255.
[107] Xi Z, Huang R, Li Z, He N, Wang T, Su E, et al. ACS Appl Mater Interfaces 2015;7:11215. https://doi.org/10.1021/acsami.5b01180.
[108] Ren C, Liu H, Lv F, Zhao W, Gao S, Yang X, et al. ACS Appl Mater Interfaces 2020;12(31):34667. https://doi.org/10.1021/acsami.0c09489.
[109] Fan W, Lu N, Huang P, Liu Y, Yang Z, Wang S, et al. Angew Chem Int Ed 2017;29:1249. https://doi.org/10.1002/ange.201610682.
[110] Fan W, Yung B, Huang P, Chen X. Chem Rev 2017;117:13566. https://doi.org/10.1021/acs.chemrev.7b00258.
[111] Liu J, Zhao X, Nie W, Yang Y, Wu C, Liu W, et al. Theranostics 2021;11:379. https://doi.org/10.7150/thno.50028.
[112] Ling D, Lee N, Hyeon T. Acc Chem Res 2015;48(5):1276. https://doi.org/10.1021/acs.accounts.5b00038.
[113] Wang Y, Jiang L, Zhang Y, Lu Y, Li Y, He Wang, et al. ACS Appl Mater Interfaces 2020;12(30):33564. https://doi.org/10.1021/acsami.0c10397.
[114] Du J, Zhang Y, Jin Z, Wu H, Cang J, Shen Y, et al. Mater Sci Eng C 2020;116:111188. https://doi.org/10.1016/j.msec.2020.111188.
[115] Weerathunge P, Pooja D, Singh M, Kulhari H, Mayes EHL, Bansal V, et al. Sens Actuators B 2019;297:126737. https://doi.org/10.1016/j.snb.2019.126737.
[116] Li B, Gong T, Xu N, Cui F, Yuan B, Yuan Q, et al. Small 2020;16(45):2003969. https://doi.org/10.1002/smll.202003969.
[117] Filippi M, Nguyen DV, Garello F, Perton F, Bégin-Colin S, Felder-Flesch D, et al. Nanoscale 2019;11:22559. https://doi.org/10.1039/c9nr08436c.
[118] Jafari S, Mahyad B, Hashemzadeh H, Janfaza S, Gholikhani T, Tayeb L. Int J Med 2020;15:3447. https://doi.org/10.2147/IJN.S249441.

[119] Yadav HM, Thorat ND, Yallapu M, Tofail SAM, Kim JS. J Mater Chem B 2022;201 (5):1461. https://doi.org/10.1039/C6TB02324J.
[120] Gea L, Hou R, Caoac C, Wu JTQ. RSC Adv 2020;10:44225. https://doi.org/10.1039/D0RA08920F.
[121] Ghaffaria SB, Sarrafzadeha MH, Fakhroueiana Z, Khorramizadeh MR. Mater Sci Eng C 2019;103:109827. https://doi.org/10.1016/j.msec.2019.109827.
[122] Briones M, Busó-Rogero C, Catalán-Gómez S, García-Mendiola T, Pariente F, Redondo-Cubero A, et al. Microchim Acta 2020;187:180. https://doi.org/10.1007/s00604-020-4137-7.
[123] Hemeg HA. Int J Nanomedicine 2017;12:8211. https://doi.org/10.2147/IJN.S132163.
[124] Ullah S, Khan SS, Ren Y, Zhang X, Qin M, Xiong X, et al. Appl Organomet Chem 2021;35:e6380. https://doi.org/10.1002/aoc.6380.
[125] Schulz M, Olubummo A, Binder H. Soft Matter 2012;8:4849. https://doi.org/10.1039/C2SM06999G.
[126] Wang L, Hu C, Shao L. Int J Nanomedicine 2017;12:1227. https://doi.org/10.2147/IJN.S121956.
[127] Abdel-Mohsen AM, Hrdina R, Burgert L, Abdel-Rahman RM, Hašová M, Šmejkalová D, et al. Carbohydr Polym 2013;92(2):1177. https://doi.org/10.1016/j.carbpol.2012.08.098.
[128] Kovačević D, Pratnekar R, Godič Torkar K, Salopek J, Dražić G, Abram A, et al. Polymers 2016;8:345. https://doi.org/10.3390/polym8100345.
[129] Bohinc K, Bajuk J, Jukić J, Abram A, Oder M, Godič Torkar K, et al. Int J Adhes Adhes 2020;103:102687. https://doi.org/10.1016/j.ijadhadh.2020.102687.
[130] Bohinc K, Kukić L, Štukelj R, Zore AM, Abram A, Klačić T, et al. Coatings 2021;11: 630. https://doi.org/10.3390/coatings11060630.
[131] Li Q, Yin Y, Cao D, Wang Y, Luan P, Sun X, et al. ACS Nano 2021;15:11992. https://doi.org/10.1021/acsnano.1c03249.
[132] Huang L, Ding L, Zhou J, Chen S, Chen F, Zhao C, et al. Biosens Bioelectron 2021; 171:112685. https://doi.org/10.1016/j.bios.2020.112685.
[133] MacPhee J, Kinyenye T, MacLean BJ, Bertin E, Hallett-Tapley GL. Ind Eng Chem Res 2021;60:17390. https://doi.org/10.1021/acs.iecr.1c03165.
[134] Huang C, Wen T, Shi FJ, Zeng XY, Jiao YJ. ACS Omega 2020;5(21):12550. https://doi.org/10.1021/acsomega.0c01554.
[135] Qiu G, Gai Z, Tao Y, Schmitt J, Kullak-Ublick GA, Wang J. ACS Nano 2020;14(5): 5268. https://doi.org/10.1021/acsnano.0c02439.
[136] Kumar A, Sharma A, Chen Y, Jones MM, Vanyo ST, Li C, et al. Adv Funct Mater 2020;2008054:1. https://doi.org/10.1002/adfm.202008054.
[137] Behzadinasab S, Chin A, Hosseini M, Poon L, Ducker WA. ACS Appl Mater Interfaces 2020;12(31):34723. https://doi.org/10.1021/acsami.0c11425.
[138] Khaiboullina S, Uppal T, Dhabarde N, Subramanian VR, Verma SC. Viruses 2020; 13:1. https://doi.org/10.3390/v13010019.
[139] Tong Y, Shi G, Hu G, Hu X, Han L, Xie X, et al. Chem Eng J 2021;414:128788. https://doi.org/10.1016/j.cej.2021.128788.